Martin Wegener

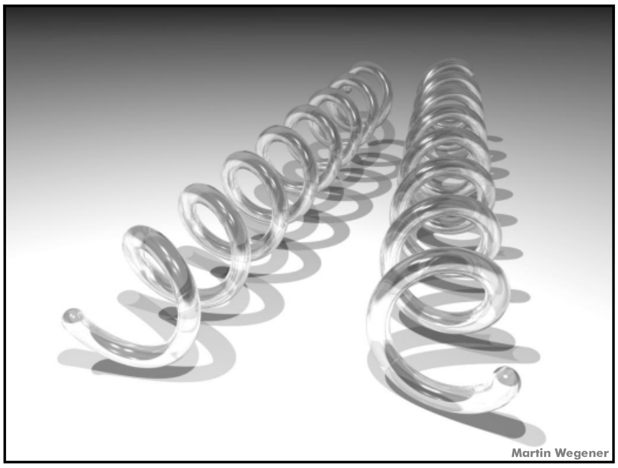

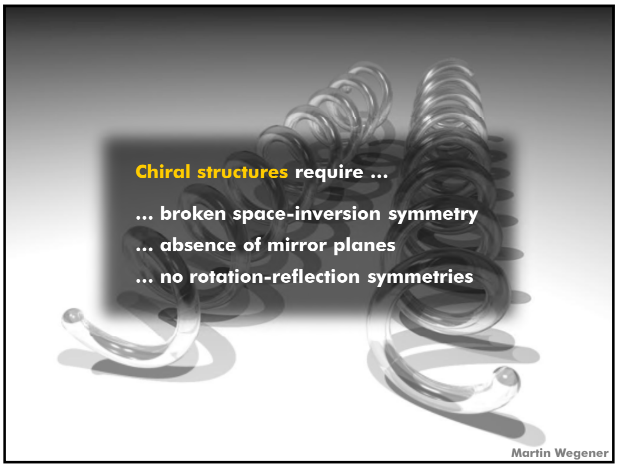

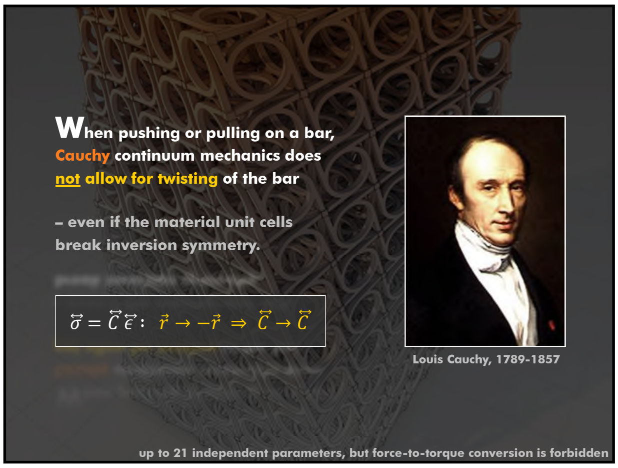

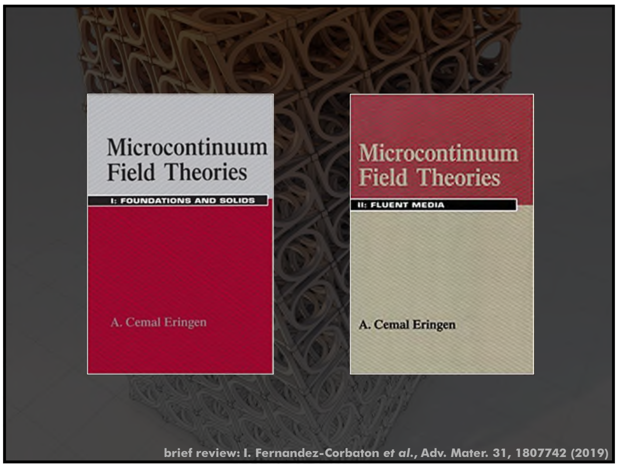

electromagnetic continua

$$D_i = \epsilon_0 \epsilon_{ij} E_j + \frac{\mathrm{i}}{c_0} \xi_{ij} H_j$$

$$B_i = \frac{1}{\mathrm{i} c_0} \xi_{ji} E_j + \mu_0 \mu_{ij} H_j$$

continuum mechanics

$$\sigma_{ij} = C_{ijkl} \epsilon_{kl} + B_{lkij} \varphi_{kl}$$

$$m_{ij} = B_{ijkl} \epsilon_{kl} + A_{ijkl} \varphi_{kl}$$

complete if $a \ll L$ **and** $a \ll \lambda$

Einstein summation convention, reciprocity assumed

electromagnetic continua

$$D_i = \epsilon_0 \epsilon_{ij} E_j + \frac{i}{c_0}\xi_{ij} H_j$$

$$B_i = \frac{1}{ic_0}\xi_{ji} E_j + \mu_0 \mu_{ij} H_j$$

continuum mechanics

$$\sigma_{ij} = C_{ijkl}\epsilon_{kl} + B_{lkij}\varphi_{kl}$$

$$m_{ij} = B_{ijkl}\epsilon_{kl} + A_{ijkl}\varphi_{kl}$$

Einstein summation convention, reciprocity assumed

electromagnetic continua

$$D_i = \epsilon_0 \epsilon_{ij} E_j + \frac{i}{c_0}\xi_{ij} H_j$$

$$B_i = \frac{1}{ic_0}\xi_{ji} E_j + \mu_0 \mu_{ij} H_j$$

continuum mechanics

$$\sigma_{ij} = C_{ijkl}\epsilon_{kl} + B_{lkij}\varphi_{kl}$$

$$m_{ij} = B_{ijkl}\epsilon_{kl} + A_{ijkl}\varphi_{kl}$$

$\epsilon_{ij} = \mu_{ij}$: **dual & helicity preserving media**

Einstein summation convention, reciprocity assumed

electromagnetic continua

$$D_i = \epsilon_0 \epsilon_{ij} E_j + \frac{i}{c_0}\xi_{ij} H_j$$

$$B_i = \frac{1}{ic_0}\xi_{ji} E_j + \mu_0 \mu_{ij} H_j$$

continuum mechanics

$$\sigma_{ij} = C_{ijkl}\epsilon_{kl} + B_{lkij}\varphi_{kl}$$

$$m_{ij} = B_{ijkl}\epsilon_{kl} + A_{ijkl}\varphi_{kl}$$

cross-terms nonzero if medium is chiral

Einstein summation convention, reciprocity assumed

Martin Wegener

Independent Parameters

	Cauchy elasticity	micropolar elasticity
isotropic	2	9
cubic chiral*	3	12
triclinic	21	196

*pentagon ikosi-tetrahedral point group, Schoenflies symbol O, Hermann-Mauguin symbol 432

3D Chiral Unit Cell

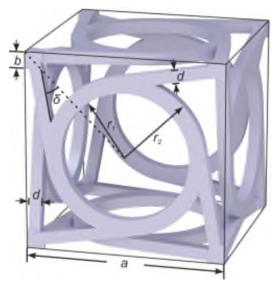

T. Frenzel *et al.*, Science 358, 1072 (2017)

3D Chiral Unit Cell

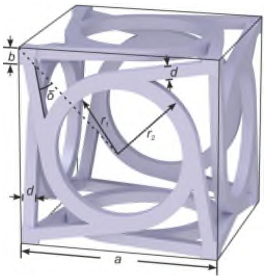

make r_2 as large as possible, use maximum geometrically possible angle

Mechanism

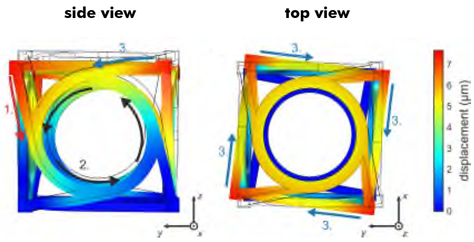

note that the center of mass does not move in *xy*-plane

3D Chiral Lattice

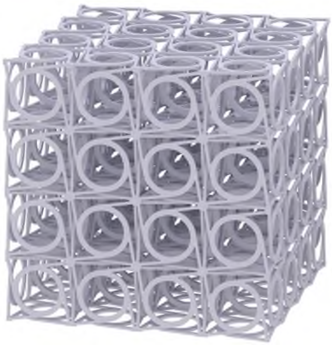

T. Frenzel *et al.*, Science 358, 1072 (2017)

Intuitive Picture

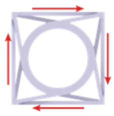

Tobias Frenzel

Intuitive Picture

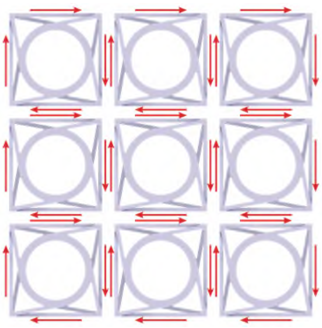

Tobias Frenzel

Intuitive Picture

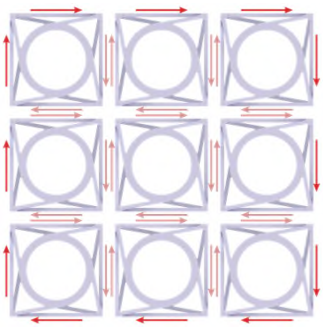

Tobias Frenzel

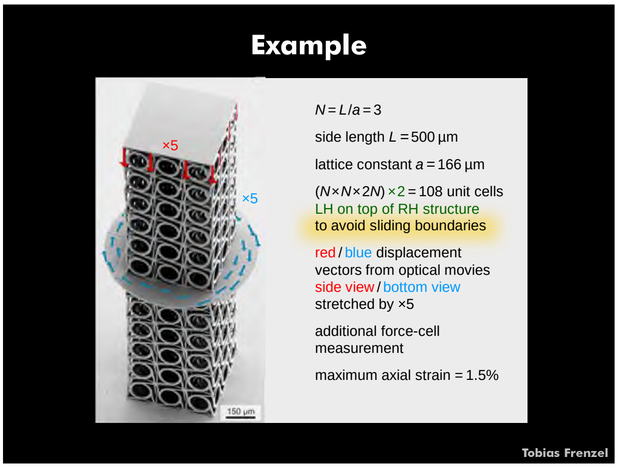
Example
×5
×5
150 µm
N = L/a = 3
side length L = 500 µm
lattice constant a = 166 µm
(N×N×2N) ×2 = 108 unit cells
LH on top of RH structure
to avoid sliding boundaries
red / blue displacement
vectors from optical movies
side view / bottom view
stretched by ×5
additional force-cell
measurement
maximum axial strain = 1.5%
Tobias Frenzel

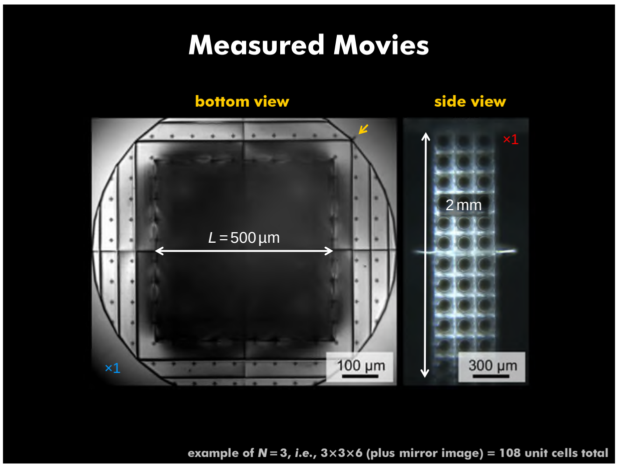
Measured Movies
bottom view
side view
L = 500 µm
×1
100 µm
×1
2 mm
300 µm
example of N = 3, i.e., 3×3×6 (plus mirror image) = 108 unit cells total

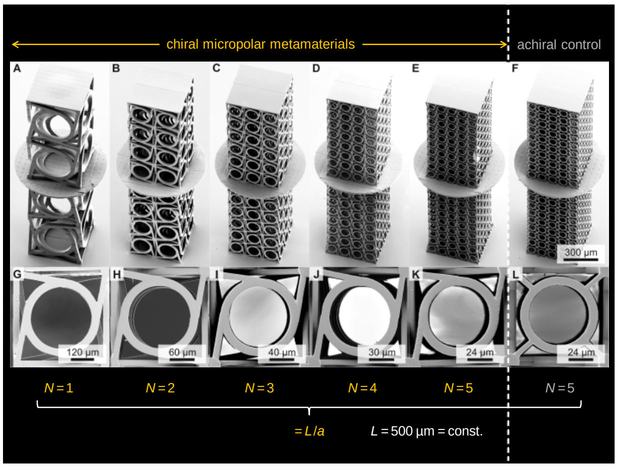
chiral micropolar metamaterials
achiral control
A
B
C
D
E
F
300 µm
G
H
I
J
K
L
120 µm
60 µm
40 µm
30 µm
24 µm
24 µm
N = 1
N = 2
N = 3
N = 4
N = 5
N = 5
= L/a
L = 500 µm = const.

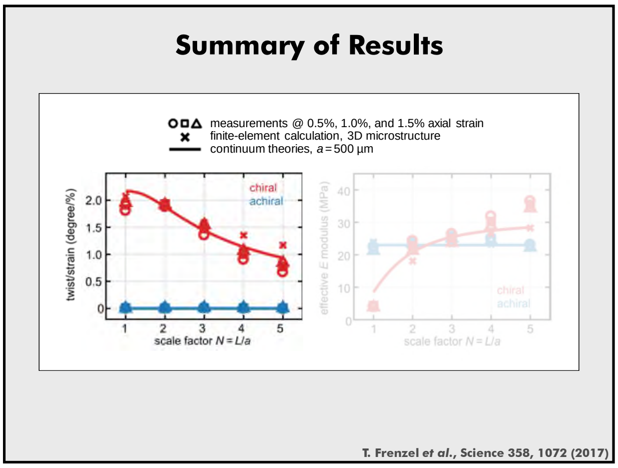
Summary of Results
measurements @ 0.5%, 1.0%, and 1.5% axial strain
finite-element calculation, 3D microstructure
continuum theories, a = 500 µm
twist/strain (degree/%)
chiral
achiral
scale factor N = L/a
effective E modulus (MPa)
chiral
achiral
scale factor N = L/a
T. Frenzel et al., Science 358, 1072 (2017)

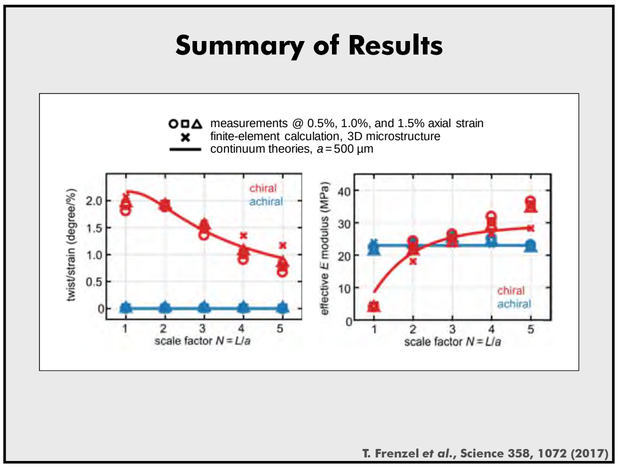
Summary of Results
measurements @ 0.5%, 1.0%, and 1.5% axial strain
finite-element calculation, 3D microstructure
continuum theories, a = 500 µm
twist/strain (degree/%)
chiral
achiral
scale factor N = L/a
effective E modulus (MPa)
chiral
achiral
scale factor N = L/a
T. Frenzel et al., Science 358, 1072 (2017)

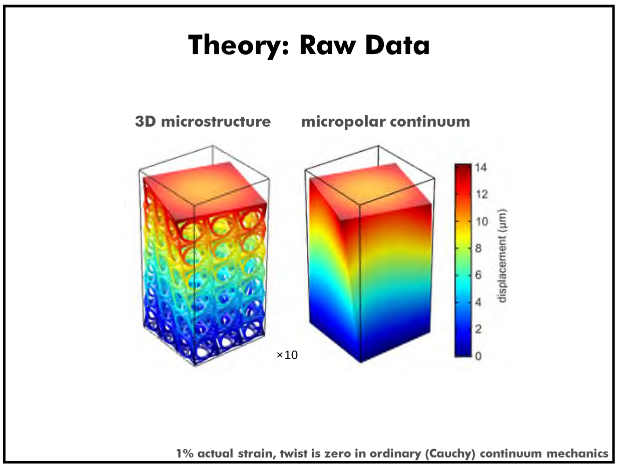
Theory: Raw Data
3D microstructure
micropolar continuum
×10
displacement (µm)
1% actual strain, twist is zero in ordinary (Cauchy) continuum mechanics

Large-Sample Limit

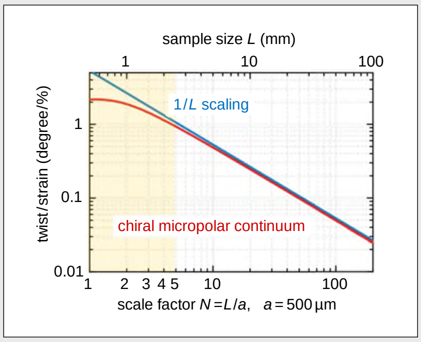

T. Frenzel *et al.*, Science 358, 1072 (2017)

Larger Length Scales?

Martin Wegener

3D Chiral Tetragonal Unit Cell

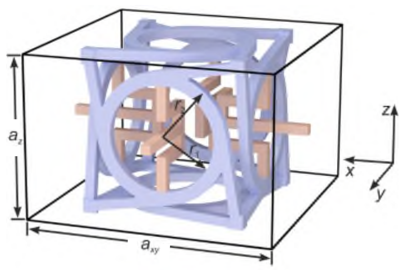

T. Frenzel *et al.*, (Nature) Commun. Mater. 2, 4 (2021)

3D Chiral Tetragonal Unit Cell

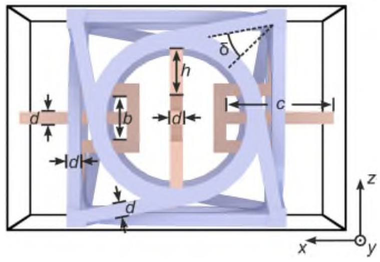

T. Frenzel *et al.*, (Nature) Commun. Mater. 2, 4 (2021)

N×*N*×(3*N*) Unit Cells; *N* = 5

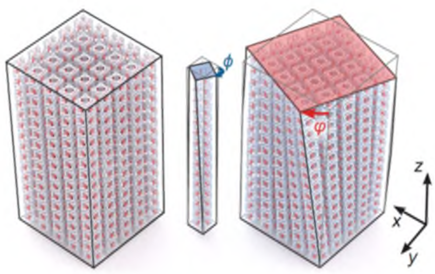

T. Frenzel *et al.*, (Nature) Commun. Mater. 2, 4 (2021)

Simple Model

T. Frenzel *et al.*, (Nature) Commun. Mater. 2, 4 (2021)

We consider three contributions to the elastic energy

$$W = W(\epsilon_{zz}, \varphi) = W_1 + W_2 + W_3$$

$$= c_1 N^3 \epsilon_{zz}^2 + c_2 N^3 \varphi^2 + c_3 N(\varphi - \phi)^2$$

$$\frac{\phi}{\epsilon_{zz}} = \gamma N$$

and search for the elastic-energy minimum

$$\frac{\partial W}{\partial \varphi} = 0 \Rightarrow \ldots$$

predetermined axial strain, linear-elastic regime, fixed sample aspect ratio

... to obtain the twist angle vs. sample size with a characteristic number or length

$$\varphi(N > 1) = \varphi(1)\frac{N N_c^2}{N^2 + N_c^2} \quad ; \quad N_c = \frac{L_c}{a_{xy}} = \sqrt{\frac{c_3}{c_2}}$$

$$\approx N \quad : \quad N \ll N_c$$

$$= N_c/2 \quad : \quad N = N_c \qquad \text{maximum}$$

$$\approx N_c^2/N \quad : \quad N \gg N_c$$

predetermined axial strain, linear-elastic regime, fixed sample aspect ratio

Simple Model

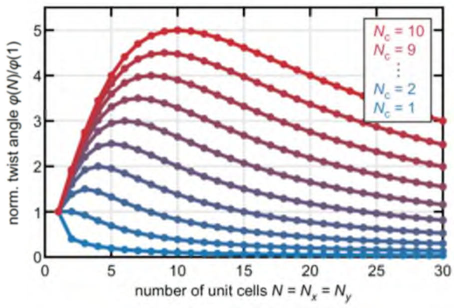

T. Frenzel *et al.*, (Nature) Commun. Mater. 2, 4 (2021)

3D Printed Samples

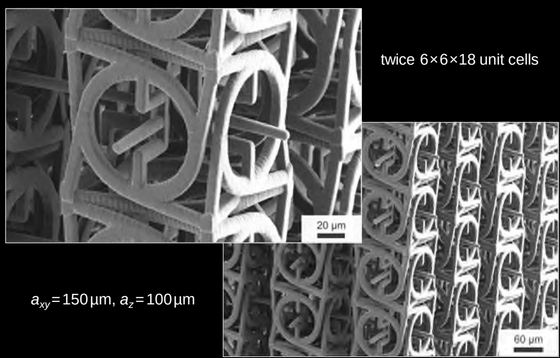

twice 6×6×18 unit cells

$a_{xy} = 150\,\mu m$, $a_z = 100\,\mu m$

T. Frenzel *et al.*, (Nature) Commun. Mater. 2, 4 (2021)

3D Printed Samples

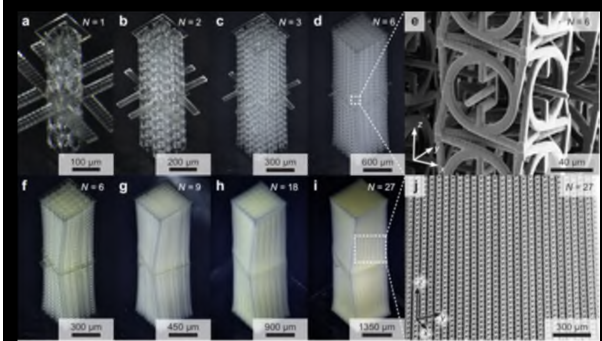

T. Frenzel *et al.*, (Nature) Commun. Mater. 2, 4 (2021)

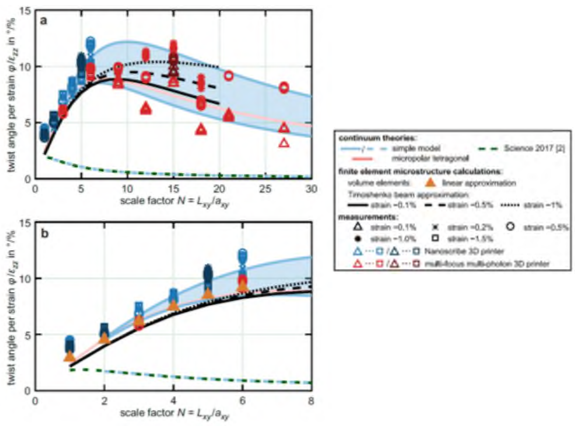

Tobias Frenzel

Martin Wegener

3D Chiral Cubic Unit Cell

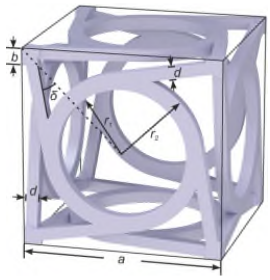

T. Frenzel *et al.*, Science 358, 1072 (2017)

Chiral Phonons

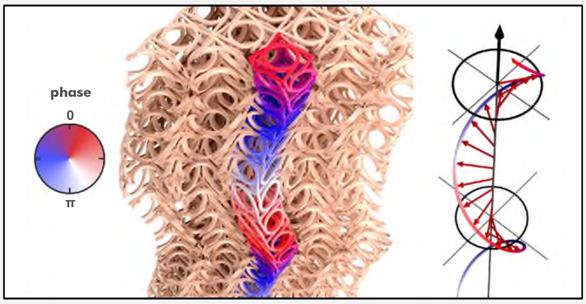

T. Frenzel *et al.*, Nature Commun. 10, 3384 (2019)

A linearly polarized wave at $z = 0$ in a chiral medium can be decomposed into circular eigenpolarizations, which propagate with different velocities along z.

This leads to the polarization rotation angle

$$\vartheta(\omega) = \left(\frac{\omega}{c_+} - \frac{\omega}{c_-}\right)\frac{L_z}{2} = \Delta k_z(\omega)\frac{L_z}{2}$$

with upper bound $|\vartheta(\omega)| \leq \frac{\pi}{2}\frac{L_z}{a}$

T. Frenzel *et al.*, Nature Commun. 10, 3384 (2019)

Acoustical Activity

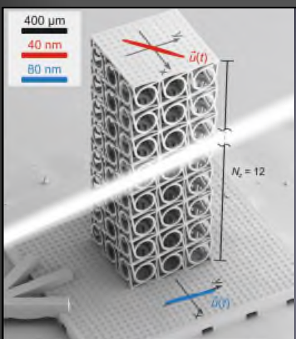

sinusoidal piezoelectric excitation @ 160 kHz

synchr. stroboscopic illumination

opt. image cross-corr. analysis (few nm noise, equiv. < 0.1 pixel)

up to 22 degrees rotation / unit cell (@ $N_x = N_y = 1$ and 180 kHz)

T. Frenzel *et al.*, Nature Commun. 10, 3384 (2019)

Experiment – Theory

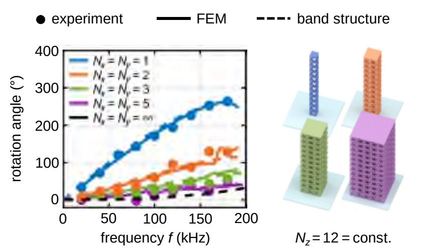

T. Frenzel *et al.*, Nature Commun. 10, 3384 (2019)

Bulk Eigenpolarizations

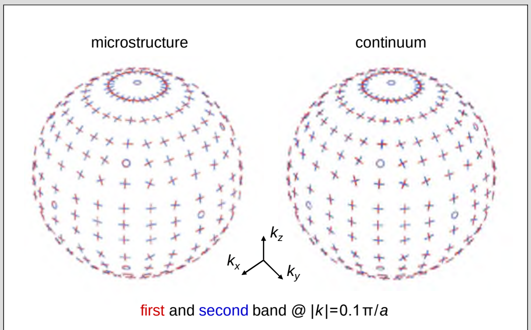

Y. Chen *et al.*, J. Mech. Phys. Solids 137, 103877 (2020)

Bulk Eigenpolarizations

Condition #1: Arrangement* is chiral.

Condition #2: Phonon wave vector is axis with *n*-fold (*n*≥3) rotational symmetry.

Condition #1 is necessary for chiral phonons.

Condition #2 together with #1 is sufficient for chiral phonons.

Condition #2 is not necessary.

* arrangement = crystal combined with phonon wave vector

Isotropic Chiral Phonons?

Martin Wegener

Martin Wegener

Using 3D Quasicrystals

Martin Wegener

3D quasi-crystals can be generated by projecting a rotated 6D simple-cubic crystal onto 3D [1].

The rotation angle is connected to the golden ratio, which can be approximated by ratios of consecutive Fibonacci numbers

$$\tau = \frac{\sqrt{5}+1}{2} = \lim_{n\to\infty} \frac{F_{n+1}}{F_n} = \frac{1}{1}, \frac{2}{1}, \frac{3}{2}, \frac{5}{3}, \frac{8}{5}, \frac{13}{8}, \frac{21}{13} \ldots$$

$$\approx 1.6180339887498948482045 86\ldots$$

[1] C. Janot, "Quasicrystals: A Primer", Clarendon Press (1998)

This approximant procedure leads to **3D crystals** based on a simple-cubic lattice with increasing **lattice constant**

$$a_{q/p} = a_{6D}\,\frac{2(q\tau + p)}{\sqrt{1+\tau^2}};\quad q = F_{n+1}, p = F_n$$

and with increasing complexity of the unit cell.

For example, the 5/3 approximant unit cell contains 2240 points (16768 meta-rods or about 3×10^5 rods).

Y. Chen *et al.*, Phys. Rev. Lett. 124, 235502 (2020)

3D Approximants

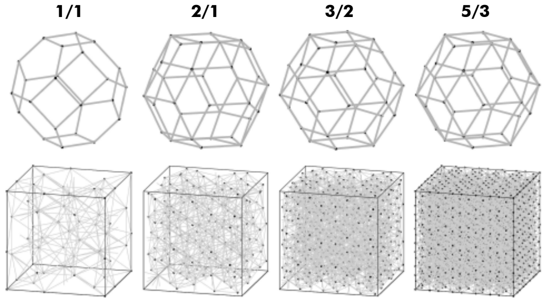

Y. Chen *et al.*, Phys. Rev. Lett. 124, 235502 (2020)

3D Chiral Architecture

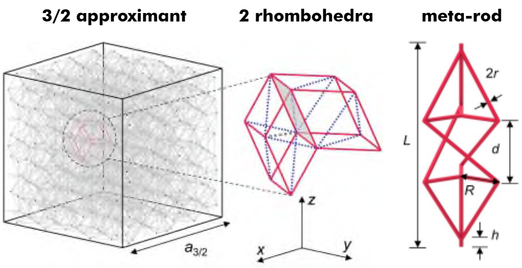

Y. Chen *et al.*, Phys. Rev. Lett. 124, 235502 (2020)

2D Penrose Tilings

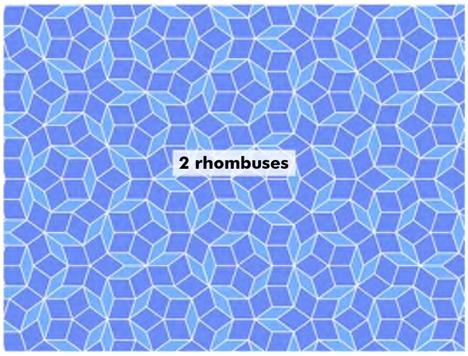

image source: https.skipython.com

3D Chiral Architecture

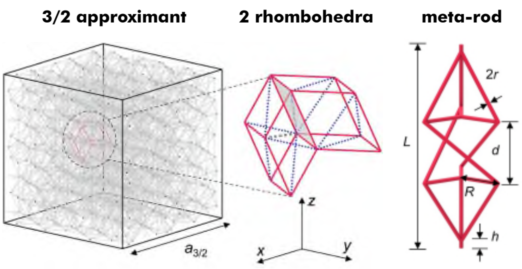

Y. Chen *et al.*, Phys. Rev. Lett. 124, 235502 (2020)

3D Chiral Architecture

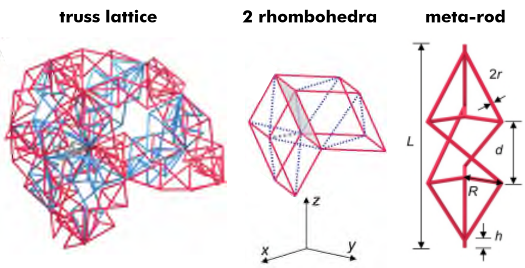

Y. Chen *et al.*, Phys. Rev. Lett. 124, 235502 (2020)

3D Unit Cells

achiral 3/2 appr. chiral 3/2 appr.

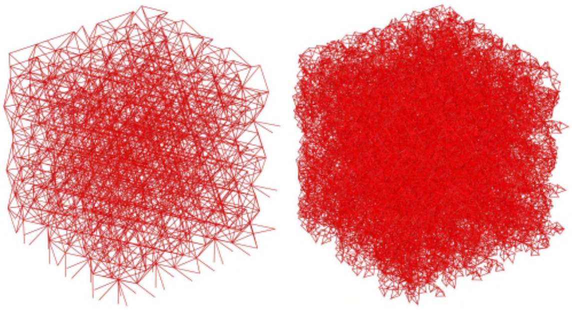

Y. Chen *et al.*, Phys. Rev. Lett. 124, 235502 (2020)

Convergence ⟶

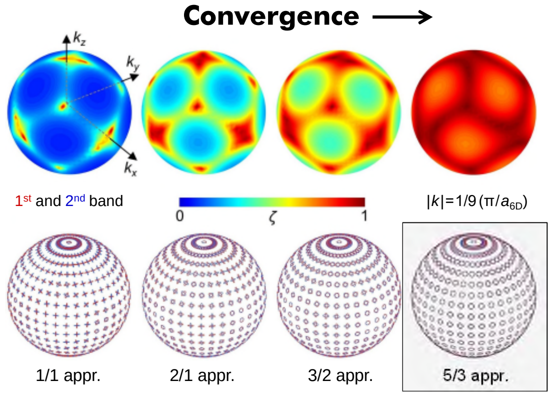

Y. Chen *et al.*, Phys. Rev. Lett. 124, 235502 (2020)

Convergence ⟶

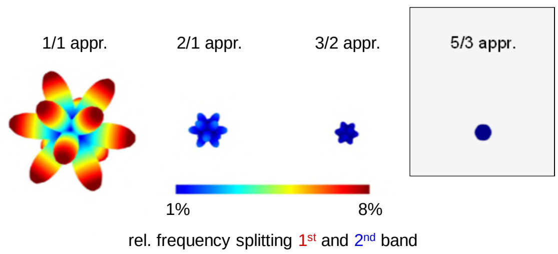

Y. Chen *et al.*, Phys. Rev. Lett. 124, 235502 (2020)

Using 3D Crystals

Martin Wegener

Isotropic (achiral) TA & LA phonons in bcc tungsten
F. H. Featherston *et al.*, Phys. Rev. 130, 1324 (1963)

Anisotropic (achiral) TA & LA phonons in bcc iron
R.E. Newnham,
Properties of Materials: Anisotropy, Symmetry, Structure
(Oxford University Press, Oxford, 2005)

accidental degeneracy in tungsten rather than *via* symmetry

1. **Make cubic ansatz (with *M* free parameters).**
2. **Do not consider all wave vectors, rather worst case, *i.e.* face diagonal (with two-fold rotational symmetry).**
3. **For this direction, minimize relative frequency splitting in the limit $k=0$ (no effect of chirality).**
4. **Inspect result for isotropy at finite *k*.**

tailored degeneracy

Yi Chen

tailored degeneracy

1. **Make cubic ansatz (with *M* free parameters).**
2. **Do not consider all wave vectors, rather worst case, *i.e.* face diagonal (with two-fold rotational symmetry).**
3. **For this direction, minimize relative frequency splitting in the limit $k=0$ (no effect of chirality).**
4. **Inspect result for isotropy at finite k.**

Yi Chen

Simple-Cubic Crystal

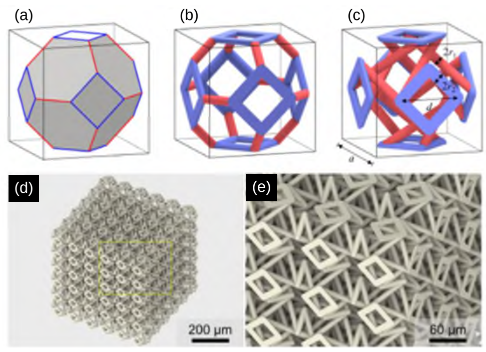

Y. Chen *et al.*, Phys. Rev. Mater. 5, 025201 (2021)

Eigenpolarizations in *k*-Space

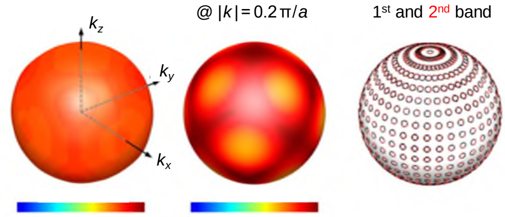

Y. Chen *et al.*, Phys. Rev. Mater. 5, 025201 (2021)

3D Printed Metamaterials

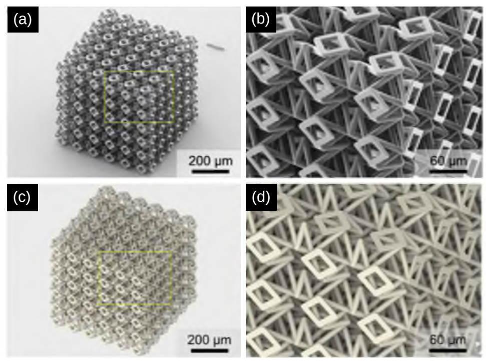

Y. Chen *et al.*, Phys. Rev. Mater. 5, 025201 (2021)

"Accidental" Degeneracy

ratio r_2/a (optimum is 0.0533) changed by relative

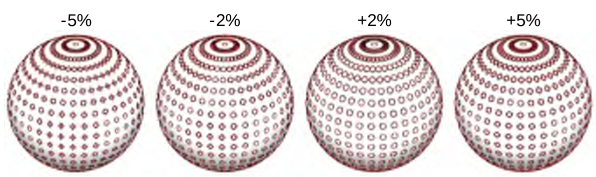

@ $|k| = 0.2\,\pi/a$ = 20% of Brillouin zone edge

1^{st} and 2^{nd} band

Y. Chen *et al.*, Phys. Rev. Mater. 5, 025201 (2021)

Alternative Ansatz

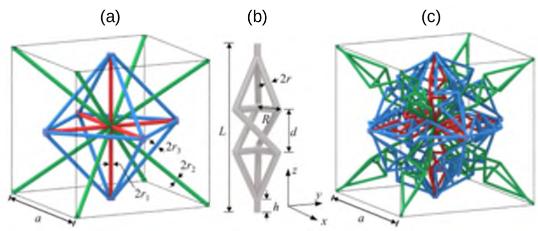

achiral simple-cubic unit cell

chiral tricilinic unit cell

Y. Chen *et al.*, Proc. Royal Soc. A 477, 20200764 (2021)

Martin Wegener

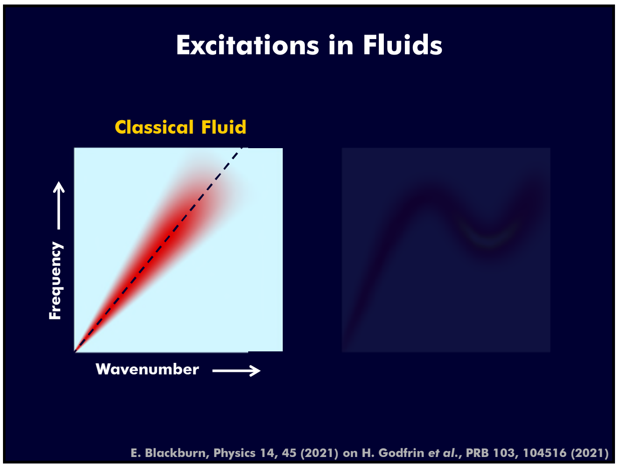

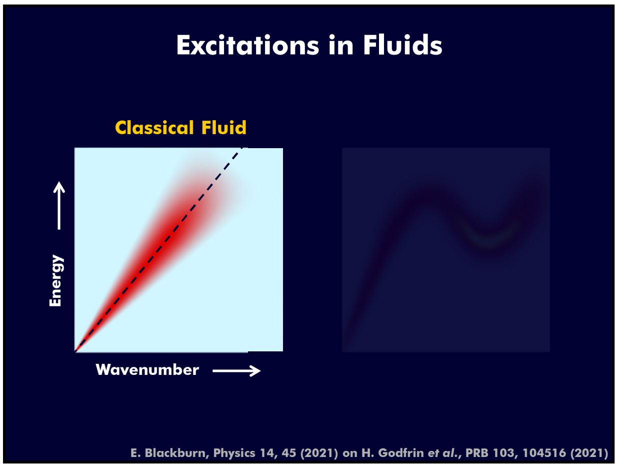

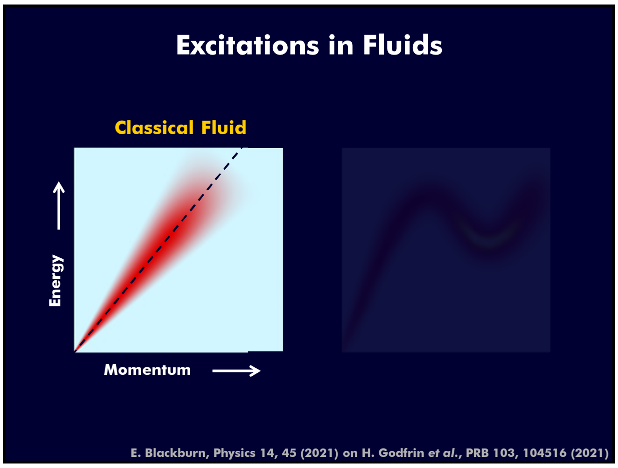

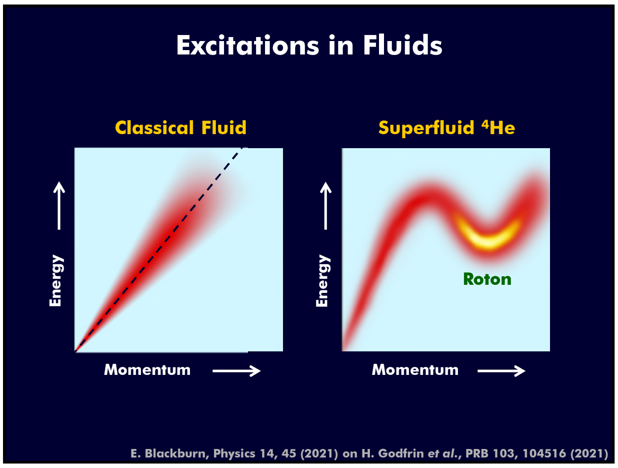

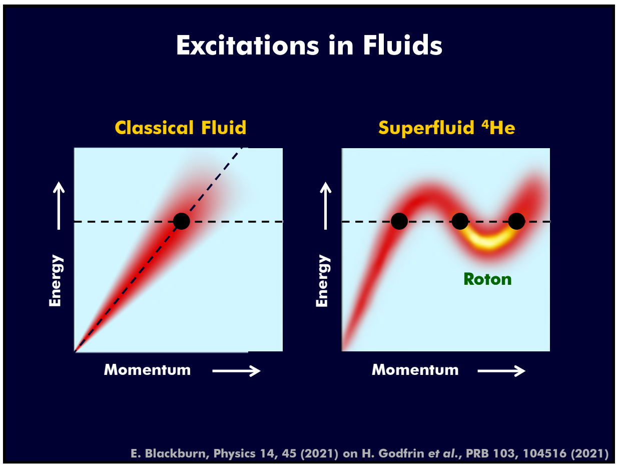

Theory of rotons in liquid ^{4}He
L. Landau, Phys. Rev. 60, 356 (1941)
R.P. Feynman, Phys. Rev. 94, 262 (1954)
H.R. Glyde and A. Griffin, Phys. Rev. Lett. 65, 1454 (1990)
G.J. Kalman *et al.*, Europhys. Lett. 90, 55002 (2010)

Rotons in inelastic neutron scattering experiments on ^{4}He
D.G. Henshaw and A.D.B. Woods, Phys. Rev. 121, 1266 (1961)
A.D.B. Woods, Phys. Rev. Lett. 14, 355 (1965)
H. Godfrin *et al.*, Phys. Rev. B 103, 104516 (2021)

Rotons in inelastic neutron scattering experiments on 2D ^{3}He
H. Godfrin *et al.*, Nature 483, 576 (2012)

Theory of roton-like dispersion in solid bcc He (111) direction
T.R. Koehler and N.R. Werthamer, Phys. Rev. A 5, 2230 (1972)

Roton Dispersion Relation

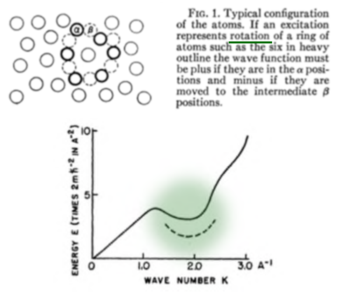

FIG. 1. Typical configuration of the atoms. If an excitation represents rotation of a ring of atoms such as the six in heavy outline the wave function must be plus if they are in the α positions and minus if they are moved to the intermediate β positions.

Rotons in Liquid ^{4}He

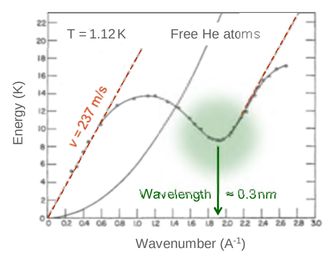

Rotons in Metamaterials?

Theory of rotons in chiral micropolar elasticity
J. Kishine *et al.*, Phys. Rev. Lett. 125, 245302 (2020)

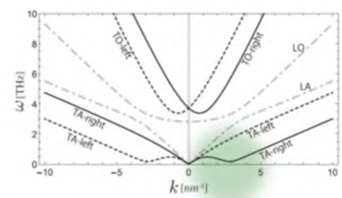

FIG. 2. Phonon dispersion curves for the chiral micropolar crystal: the longitudinal acoustic (LA) and optical (LO) branches (dash-dotted line), the transverse left-handed acoustic (TA-left) and optical (TO-left) branches (dashed line), the transverse right-handed acoustic (TA-right) and optical (TO-right) branches (solid line). Numerical values of the tensor components are chosen as $A_{33} = 0.4 \times 10^{10}$ N/m^2, $A_{66} = 4.9 \times 10^{10}$ N/m^2, $A_{69} = 4.7 \times 10^{10}$ N/m^2, $B_{33} = 1.5 \times 10^{-10}$ N, $C_{33} = 0.3$ N/m for the longitudinal modes, and $A_{44} = 0.21 \times 10^{10}$ N/m^2, $A_{55} = 0.215 \times 10^{10}$ N/m^2, $A_{47} = 0.195 \times 10^{10}$ N/m^2, $B_{44} = 1.0 \times 10^{-10}$ N, $C_{44} = 0.44$ N/m, $C_{74} = 0.36$ N/m for the transverse modes, respectively.

What Metamaterial Structure?

Martin Wegener

A Cube has 3+3 Degrees of Freedom

3 translational + 3 rotational degrees of freedom

Simple-Cubic Lattice of Cubes

Y. Chen, J.L.G. Schneider, M.F. Groß, *et al.*, Adv. Funct. Mater. 33, 2302699 (2023)

Chiral Unit Cell

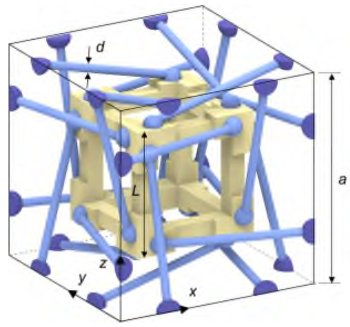

used parameters: $a = 185\,\mu m$, $d/a = 0.04$, $L/a = 0.6$

Cubic Chiral Crystal

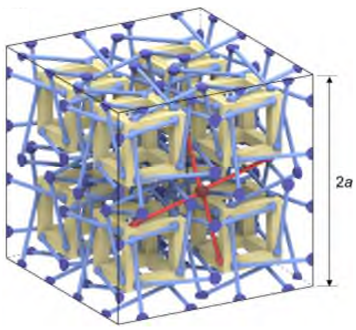

Y. Chen, J.L.G. Schneider, M.F. Groß, *et al.*, Adv. Funct. Mater. 33, 2302699 (2023)

Cubic Chiral Crystal

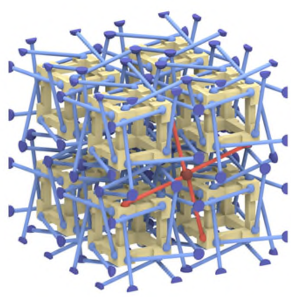

Y. Chen, J.L.G. Schneider, M.F. Groß, *et al.*, Adv. Funct. Mater. 33, 2302699 (2023)

Elastic Bulk Band Structure

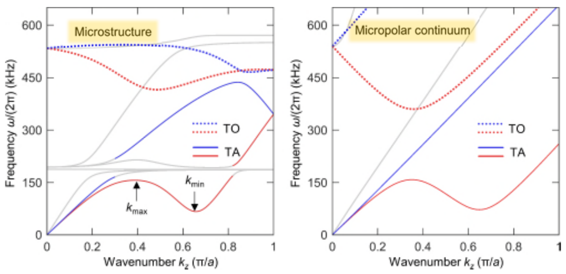

Y. Chen, J.L.G. Schneider, M.F. Groß, *et al.*, Adv. Funct. Mater. 33, 2302699 (2023)

Elastic Bulk Band Structure

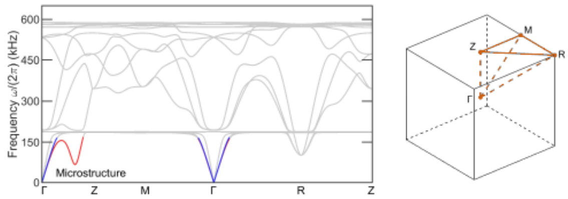

No roton along face-diagonal or body-diagonal directions

Y. Chen, J.L.G. Schneider, M.F. Groß, *et al.*, Adv. Funct. Mater. 33, 2302699 (2023)

3D μ-Printed 3×3×40 Beam

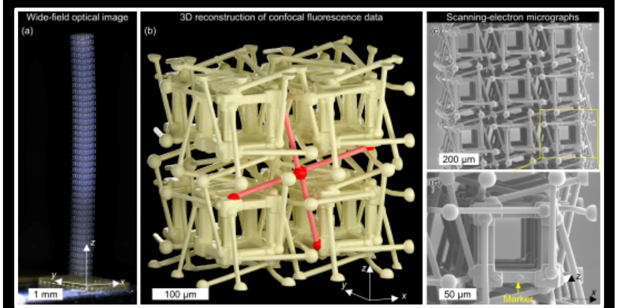

Y. Chen, J.L.G. Schneider, M.F. Groß, *et al.*, Adv. Funct. Mater. 33, 2302699 (2023)

Measurement Setup

Michael F. Groß

Home-Built Setup

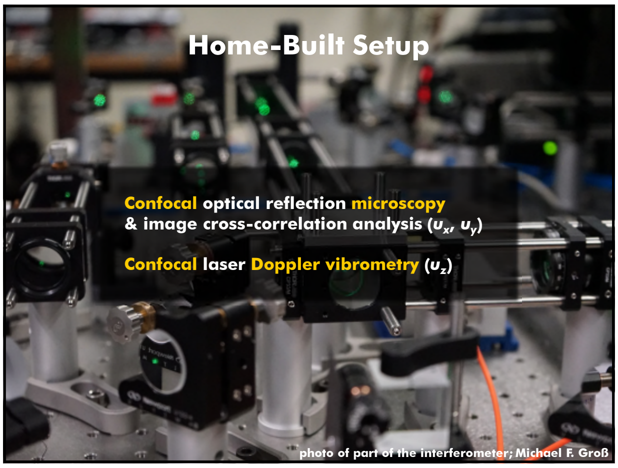

Confocal optical reflection microscopy & image cross-correlation analysis (u_x, u_y)

Confocal laser Doppler vibrometry (u_z)

photo of part of the interferometer; Michael F. Groß

Elastic Beam Band Structures

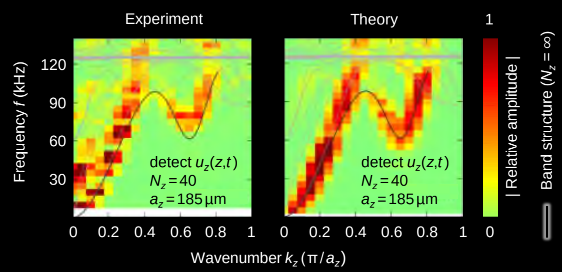

Y. Chen, J.L.G. Schneider, M.F. Groß, *et al.*, Adv. Funct. Mater. 33, 2302699 (2023)

Martin Wegener

1. Making 3D Metamaterials by 3D Laser Nanoprinting
  1.1. Using Two-Photon Absorption
  1.2. Using Two-Step Absorption
  1.3. Comparison with Other Approaches

2. Extreme Cauchy Elasticity

3. Chiral Micropolar Elasticity
  3.1. Static Case: Twists and Characteristic Length Scales
  3.2. Chiral Phonons and Acoustical Activity
  3.3. Towards Isotropic Elastic Properties
  3.4. Roton-Like Dispersion Relations

4. Nonlocal Elasticity
  4.1. Beyond-Nearest-Neighbor Interactions
  4.2. Elastic, Acoustic, and Electromagnetic Waves

5. Anomalous Frozen Evanescent Phonons
  5.1. Complex Band Structures and the Cauchy-Riemann Equations
  5.2. Examples

Martin Wegener

1D mass-and-spring model with lattice constant a

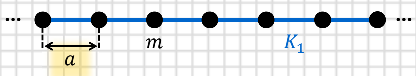

leads to $u_n(t) = \tilde{u}\cos(kna - \omega t)$ **with**

$$\omega(k) = \frac{2}{\sqrt{m}}\sqrt{K_1 \sin^2\left(\frac{ka}{2}\right)}$$

Y. Chen *et al.*, Nature Commun. 12, 3278 (2021)

1D mass-and-spring model with lattice constant a

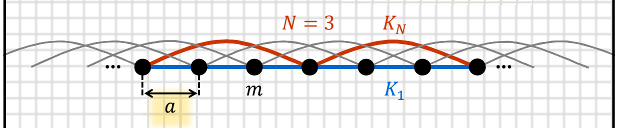

leads to $u_n(t) = \tilde{u}\cos(kna - \omega t)$ **with**

$$\omega(k) = \frac{2}{\sqrt{m}}\sqrt{K_1 \sin^2\left(\frac{ka}{2}\right) + K_N \sin^2\left(\frac{Nka}{2}\right)}$$

Y. Chen *et al.*, Nature Commun. 12, 3278 (2021)

1D mass-and-spring model with lattice constant $3a$

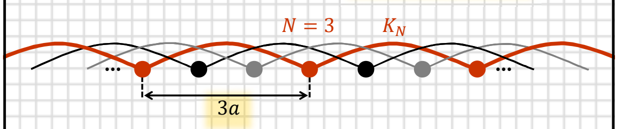

leads to $u_n(t) = \tilde{u}\cos(kna - \omega t)$ **with**

$$\omega(k) = \frac{2}{\sqrt{m}}\sqrt{K_N \sin^2\left(\frac{Nka}{2}\right)}$$

Y. Chen *et al.*, Nature Commun. 12, 3278 (2021)

1D mass-and-spring model with lattice constant a

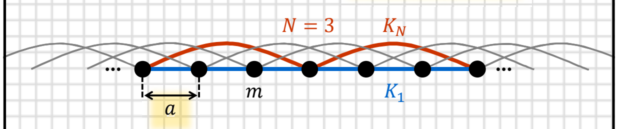

leads to $u_n(t) = \tilde{u}\cos(kna - \omega t)$ **with**

$$\omega(k) = \frac{2}{\sqrt{m}}\sqrt{K_1 \sin^2\left(\frac{ka}{2}\right) + K_N \sin^2\left(\frac{Nka}{2}\right)}$$

Y. Chen *et al.*, Nature Commun. 12, 3278 (2021)

Phonon Hybridization

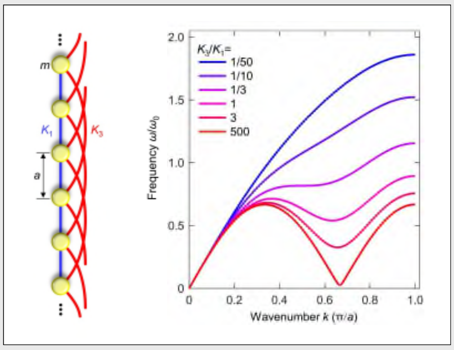

N = 3, fixed phase velocity in the long-wavelength limit

Any Dispersion Relation?

Martin Wegener

Rotons are merely a special case of designs that make use of beyond-nearest-neighbor interactions.

More generally, the acoustic-phonon dispersion can be Fourier synthesized (within the 1D toy model)

$$\omega(k) = \frac{2}{\sqrt{m}} \sqrt{\sum_{N=1}^{\infty} K_N \sin^2\left(\frac{Nka}{2}\right)} \qquad |k| \leq \frac{\pi}{a}$$

N-th nearest-neighbor Hooke's spring constant

Y. Chen *et al.*, Nature Commun. 12, 3278 (2021)

Rotons are merely a special case of designs that make use of beyond-nearest-neighbor interactions.

More generally, the acoustic-phonon dispersion can be Fourier synthesized (within the 1D toy model)

$$\omega(k) = \frac{2}{\sqrt{m}} \sqrt{\sum_{N=1}^{\infty} K_N \sin^2\left(\frac{Nka}{2}\right)} \qquad |k| \leq \frac{\pi}{a}$$

N-th nearest-neighbor Hooke's spring constant

also see: L. Brillouin, "Wave propagation in periodic structures …", Dover Pubns., 1946

Rotons are merely a special case of designs that make use of beyond-nearest-neighbor interactions.

More generally, the acoustic-phonon dispersion can be Fourier synthesized (within the 1D toy model)

$$\Rightarrow \omega^2(k) = \sum_{N=0}^{\infty} c_N \cos(Nka) \geq 0; \quad |k| \leq \frac{\pi}{a}$$

$$c_0 = \frac{2}{m} \sum_{N=1}^{\infty} K_N\,; \quad c_{N\geq 1} = -\frac{2}{m} K_N \quad \Rightarrow \omega(k \to 0) \propto k$$

also see: A. Kazemi *et al.*, Phys. Rev. Lett. 131, 176101 (2023)

Hooke's Law has Issues

Martin Wegener

When it comes to designing actual metamaterial structures, be aware that **Hooke's law** …

… accounts for only a **single degree of freedom**

… and **violates causality**.

Effective-Medium Description

The simple 1D mass-and-spring toy model

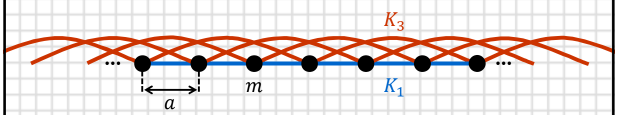

follows Newton's equation of motion

$$m\frac{\partial^2 u_n}{\partial t^2} = +K_1(u_{n+1} - 2u_n + u_{n-1})$$
$$+K_3(u_{n+3} - 2u_n + u_{n-3})$$

The simple 1D mass-and-spring toy model

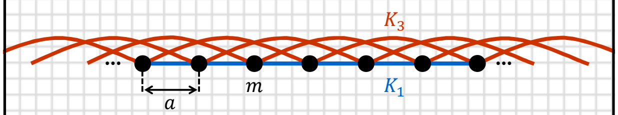

follows Newton's equation of motion

$$m\frac{\partial^2 u_n}{\partial t^2} = +K_1 a^2 \frac{u_{n+1} - 2u_n + u_{n-1}}{a^2}$$
$$+K_3(u_{n+3} - 2u_n + u_{n-3})$$

The simple 1D mass-and-spring toy model

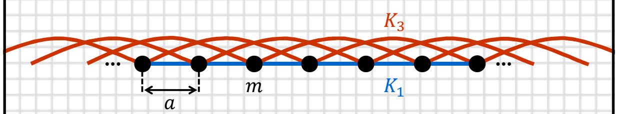

follows Newton's equation of motion

$$m\frac{\partial^2 u_n}{\partial t^2} = +K_1 a^2 \frac{u_{n+1} - 2u_n + u_{n-1}}{a^2} \approx K_1 a^2 \frac{\partial^2 u}{\partial x^2}$$
$$+K_3(u_{n+3} - 2u_n + u_{n-3})$$

The simple 1D mass-and-spring toy model

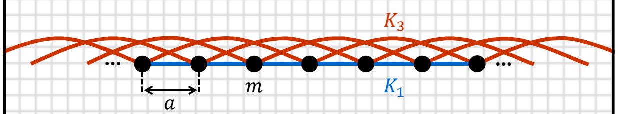

follows Newton's equation of motion

$$m\frac{\partial^2 u_n}{\partial t^2} = +K_1 a^2 \frac{u_{n+1} - 2u_n + u_{n-1}}{a^2}$$
$$+K_3(u_{n+3} - 2u_n + u_{n-3})$$

The simple 1D mass-and-spring toy model

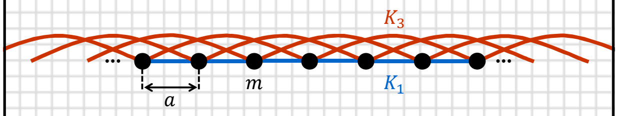

follows Newton's equation of motion

$$m\frac{\partial^2 u_n}{\partial t^2} = +K_1 a^2 \frac{u_{n+1} - 2u_n + u_{n-1}}{a^2}$$
$$+K_3(u_{n+3} - 2u_n + u_{n-3})$$

Higher-order difference quotients can be approximated by higher-order derivatives.

Here, only even orders occur, for which we have

$$\frac{\partial^m u}{\partial x^m} \approx \frac{1}{a^m}\sum_{j=0}^{m}(-1)^j \frac{m!}{j!\,(m-j)!}\, u_{n+j-\frac{m}{2}}$$

This allows us to rewrite the term

$$+K_3(u_{n+3} - 2u_n + u_{n-3}) \qquad m = 2, 4, 6$$

...

... such that, in the continuum limit, we obtain the modified wave equation for *N*=3

$$m\frac{\partial^2 u}{\partial t^2} = A_2\frac{\partial^2 u}{\partial x^2} + A_4\frac{\partial^4 u}{\partial x^4} + A_6\frac{\partial^6 u}{\partial x^6} \qquad a \to 0$$

with coefficients

$$A_2 = K_1 a^2 + 9K_3 a^2$$
$$A_4 = 6K_3 a^4$$
$$A_6 = K_3 a^6$$

... such that, in the continuum limit, we obtain the modified wave equation for *N*=3

$$m\frac{\partial^2 u}{\partial t^2} = A_2\frac{\partial^2 u}{\partial x^2} + A_4\frac{\partial^4 u}{\partial x^4} + A_6\frac{\partial^6 u}{\partial x^6} \qquad a \to 0$$

enabling roton-like dispersion relations

$$\omega(k) = \frac{1}{\sqrt{m}}\sqrt{A_2 k^2 - A_4 k^4 + A_6 k^6}$$

Elastic Waves

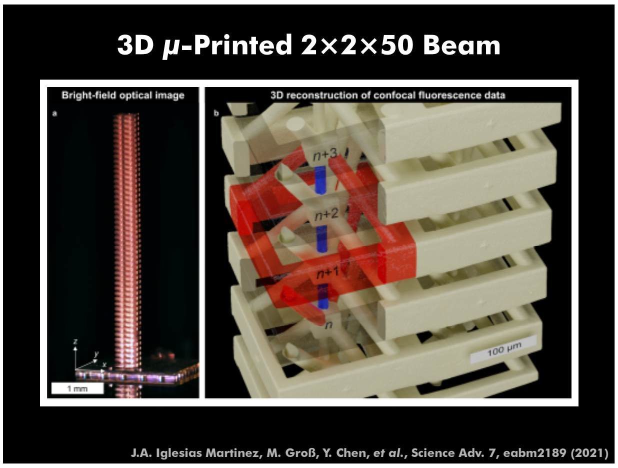
3D μ-Printed 2×2×50 Beam
Bright-field optical image
3D reconstruction of confocal fluorescence data
n+3
n+2
n+1
n
100 μm
1 mm
J.A. Iglesias Martinez, M. Groß, Y. Chen, et al., Science Adv. 7, eabm2189 (2021)

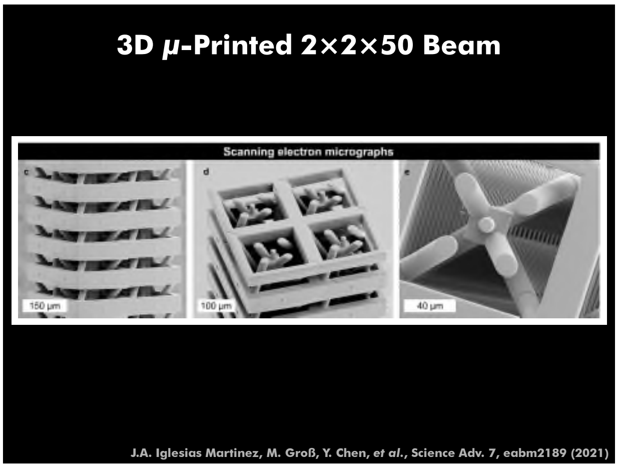
3D μ-Printed 2×2×50 Beam
Scanning electron micrographs
150 μm
100 μm
40 μm
J.A. Iglesias Martinez, M. Groß, Y. Chen, et al., Science Adv. 7, eabm2189 (2021)

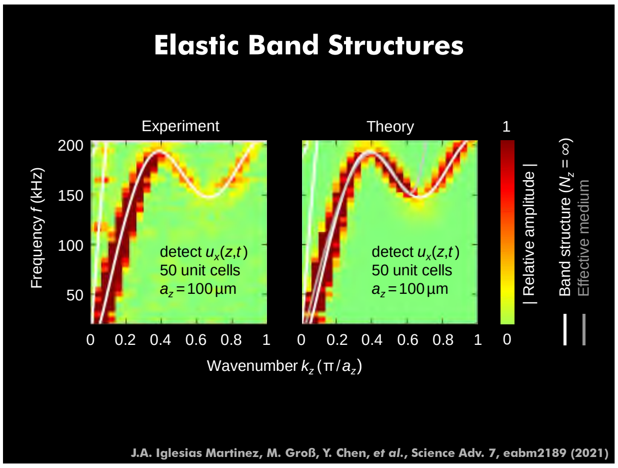
Elastic Band Structures
Experiment
Theory
Frequency f (kHz)
detect u_x(z,t)
50 unit cells
a_z = 100 μm
Wavenumber k_z (π/a_z)
| Relative amplitude |
Band structure (N_z = ∞)
Effective medium
J.A. Iglesias Martinez, M. Groß, Y. Chen, et al., Science Adv. 7, eabm2189 (2021)


Acoustic Waves
Martin Wegener

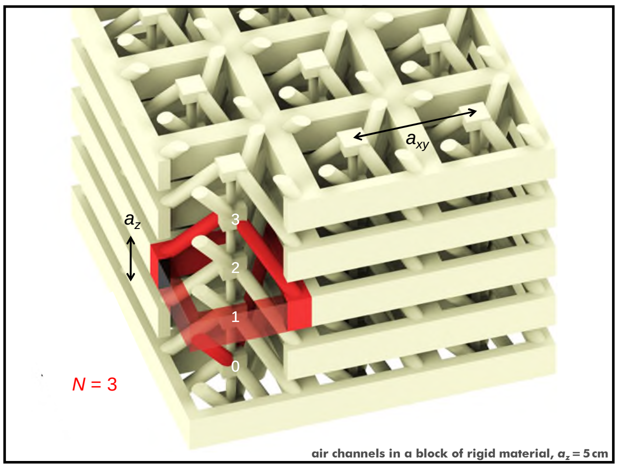
a_xy
a_z
N = 3
air channels in a block of rigid material, a_z = 5 cm

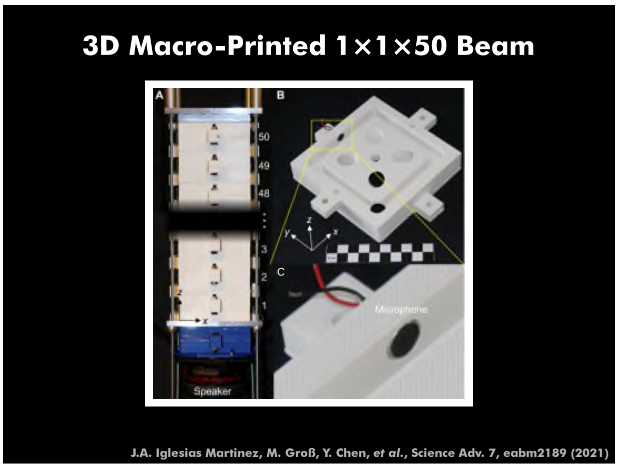
3D Macro-Printed 1×1×50 Beam
A
B
C
50
49
48
3
2
Microphone
Speaker
J.A. Iglesias Martinez, M. Groß, Y. Chen, et al., Science Adv. 7, eabm2189 (2021)

Acoustic Band Structures

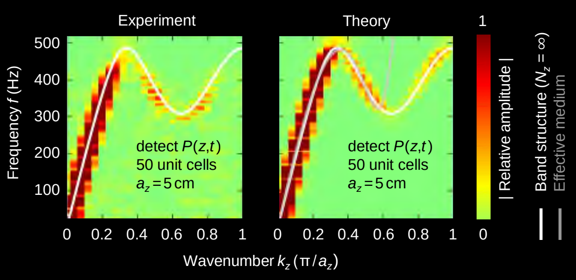

J.A. Iglesias Martinez, M. Groß, Y. Chen, *et al.*, Science Adv. 7, eabm2189 (2021)

N>3 Actually Possible?

K. Wang, Y. Chen, *et al.*, Commun. Mater. 3, 35 (2022)

2D Lattice (*N*=3)

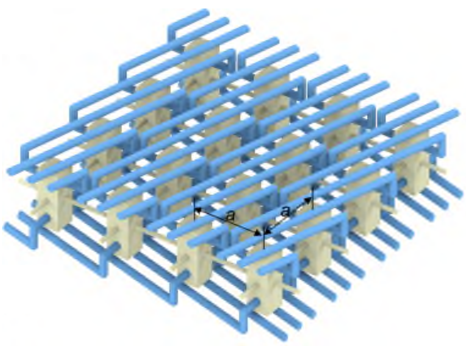

K. Wang, Y. Chen, *et al.*, Commun. Mater. 3, 35 (2022)

One Unit Cell (*N*=3)

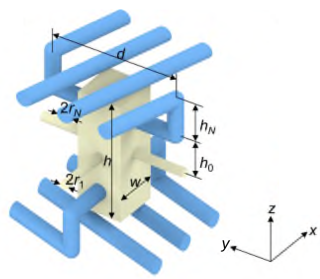

K. Wang, Y. Chen, *et al.*, Commun. Mater. 3, 35 (2022)

Different Orders

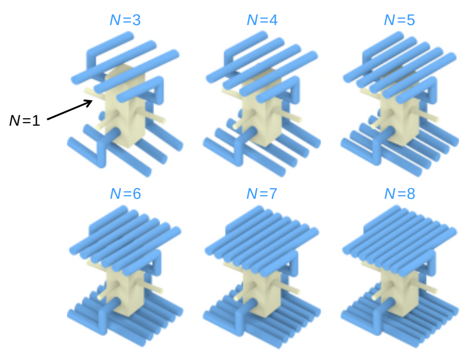

K. Wang, Y. Chen, *et al.*, Commun. Mater. 3, 35 (2022)

N=1 and *N*=3 and *N*=5

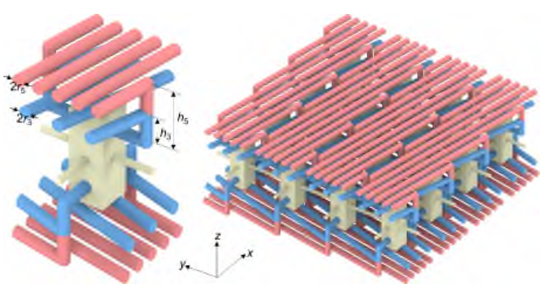

K. Wang, Y. Chen, *et al.*, Commun. Mater. 3, 35 (2022)

N=1 and N=3 and N=5

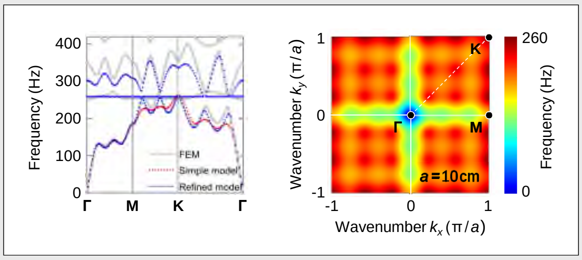

K. Wang, Y. Chen, *et al.*, Commun. Mater. 3, 35 (2022)

Electromagnetic Waves

Martin Wegener

BNC Cables as Connections

BNC = Bayonet Neill–Concelman; image source: www.llt-versand.de

BNC-Cable Metamaterial

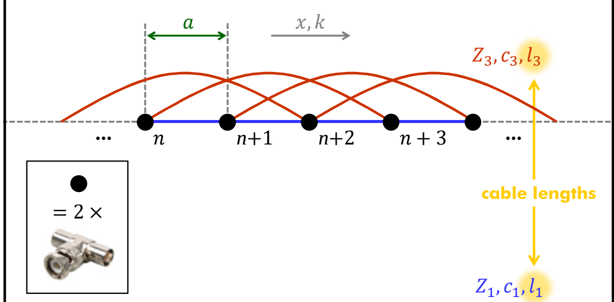

Y. Chen *et al.*, Adv. Mater. 35, 2209988 (2023)

BNC-Cable Metamaterial

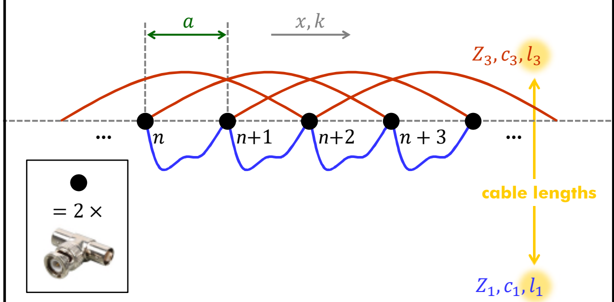

Y. Chen *et al.*, Adv. Mater. 35, 2209988 (2023)

BNC-Cable Metamaterial

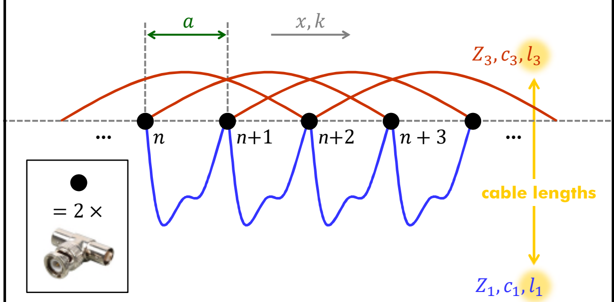

Y. Chen *et al.*, Adv. Mater. 35, 2209988 (2023)

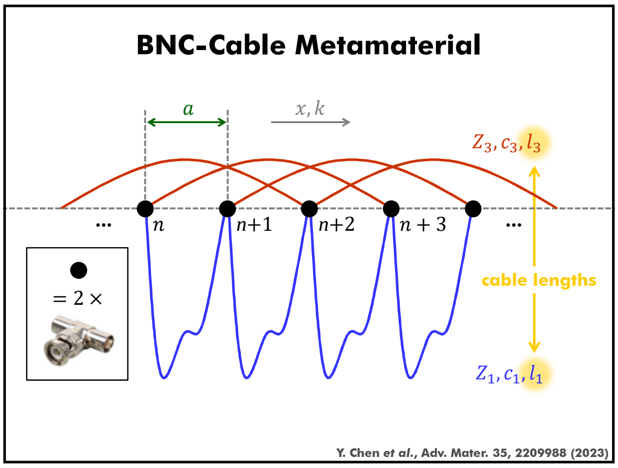
BNC-Cable Metamaterial
a
x, k
Z_3, c_3, l_3
n
n+1
n+2
n + 3
...
= 2 ×
cable lengths
Z_1, c_1, l_1
Y. Chen et al., Adv. Mater. 35, 2209988 (2023)

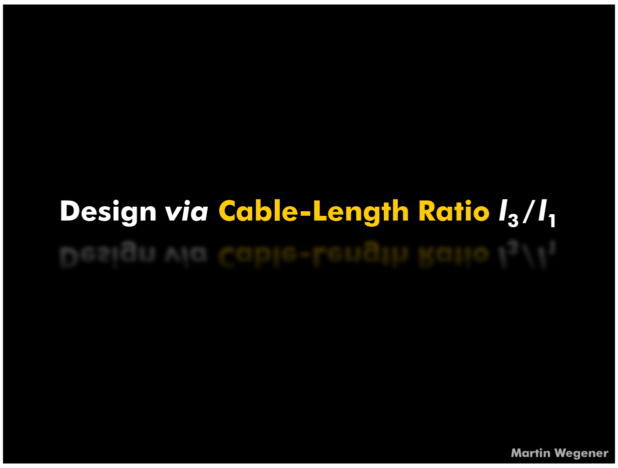
Design via Cable-Length Ratio l_3/l_1
Martin Wegener

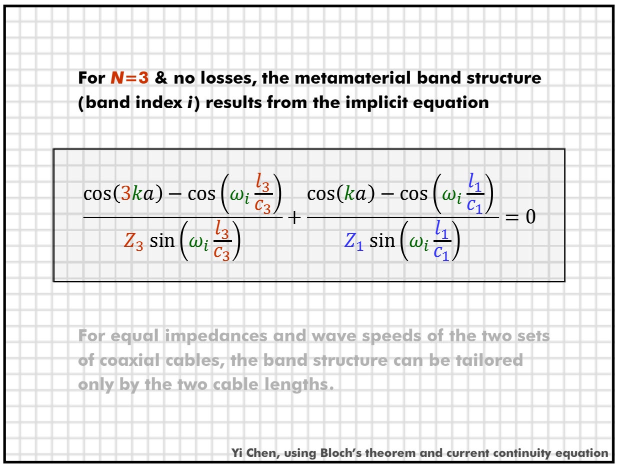
For N=3 & no losses, the metamaterial band structure (band index i) results from the implicit equation
$\frac{\cos(3ka) - \cos\left(\omega_i \frac{l_3}{c_3}\right)}{Z_3 \sin\left(\omega_i \frac{l_3}{c_3}\right)} + \frac{\cos(ka) - \cos\left(\omega_i \frac{l_1}{c_1}\right)}{Z_1 \sin\left(\omega_i \frac{l_1}{c_1}\right)} = 0$
For equal impedances and wave speeds of the two sets of coaxial cables, the band structure can be tailored only by the two cable lengths.
Yi Chen, using Bloch's theorem and current continuity equation

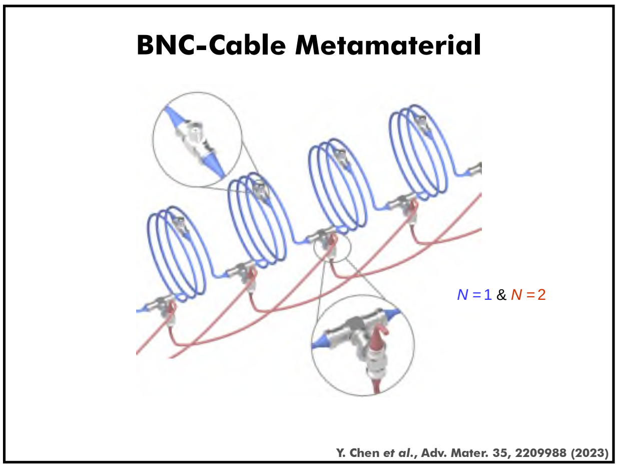
BNC-Cable Metamaterial
N = 1 & N = 2
Y. Chen et al., Adv. Mater. 35, 2209988 (2023)

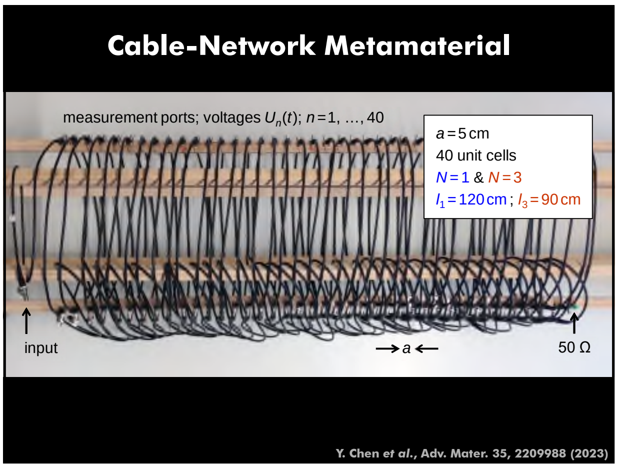
Cable-Network Metamaterial
measurement ports; voltages $U_n(t)$; n = 1, ..., 40
a = 5 cm
40 unit cells
N = 1 & N = 3
l_1 = 120 cm ; l_3 = 90 cm
input
→ a ←
50 Ω
Y. Chen et al., Adv. Mater. 35, 2209988 (2023)

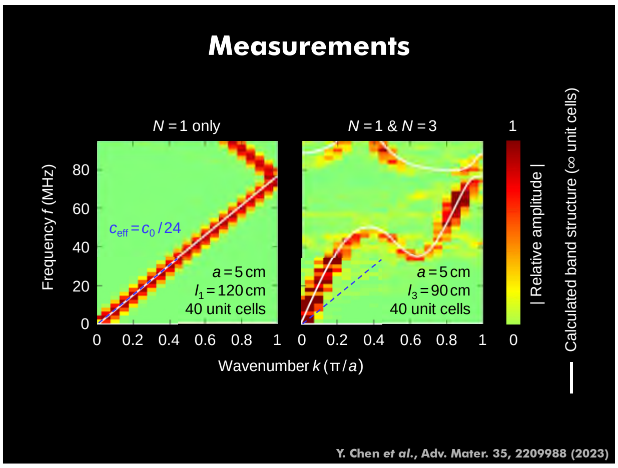
Measurements
N = 1 only
N = 1 & N = 3
Frequency f (MHz)
80
60
40
20
0
$c_{eff} = c_0 / 24$
a = 5 cm
l_1 = 120 cm
40 unit cells
a = 5 cm
l_3 = 90 cm
40 unit cells
0 0.2 0.4 0.6 0.8 1
0 0.2 0.4 0.6 0.8 1
Wavenumber k (π / a)
1
0
| Relative amplitude |
Calculated band structure (∞ unit cells)
Y. Chen et al., Adv. Mater. 35, 2209988 (2023)

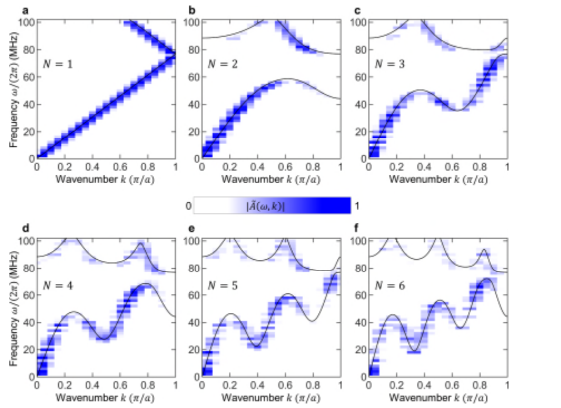

Y. Chen *et al.*, Adv. Mater. 35, 2209988 (2023)

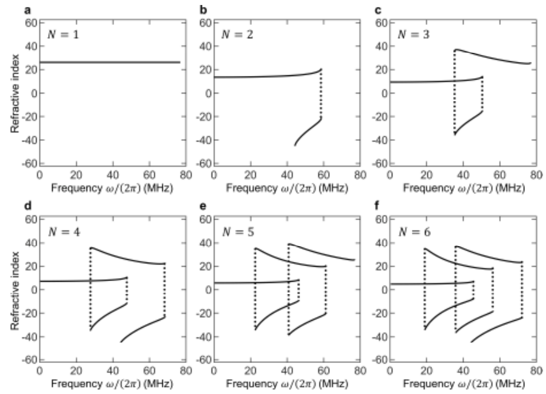

Y. Chen *et al.*, Adv. Mater. 35, 2209988 (2023)

More Possibilities

Martin Wegener

For *N*=3 & no losses, the metamaterial band structure (band index *i*) results from the implicit equation

$$\frac{\cos(3ka)-\cos\left(\omega_i \frac{l_3}{c_3}\right)}{Z_3 \sin\left(\omega_i \frac{l_3}{c_3}\right)} + \frac{\cos(ka)-\cos\left(\omega_i \frac{l_1}{c_1}\right)}{Z_1 \sin\left(\omega_i \frac{l_1}{c_1}\right)} = 0$$

For equal impedances and wave speeds of the two sets of coaxial cables, the band structure can be tailored only by the two cable lengths.

Yi Chen, using Bloch's theorem and current continuity equation

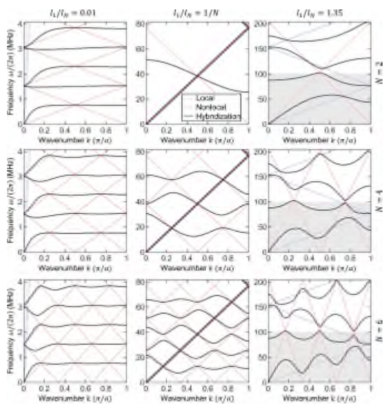

Y. Chen *et al.*, Adv. Mater. 35, 2209988 (2023)

Martin Wegener

Static Consequences?

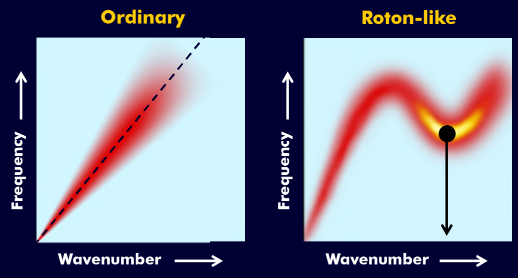

Martin Wegener

Martin Wegener

Mathematically, a phonon dispersion relation as, e.g.,

$$\omega(k) = \frac{2}{\sqrt{m}} \sqrt{K_1 \sin^2\left(\frac{ka}{2}\right) + K_N \sin^2\left(\frac{Nka}{2}\right)}$$

has eigensolutions with complex spatial frequency

$$k = \mathrm{Re}(k) + \mathrm{i}\,\mathrm{Im}(k)$$

also in the static case, with eigenvalue $\omega(k) = 0$.

Y. Chen, J.L.G. Schneider, *et al.*, in preparation (2023)

Complex Phonon Band Structure

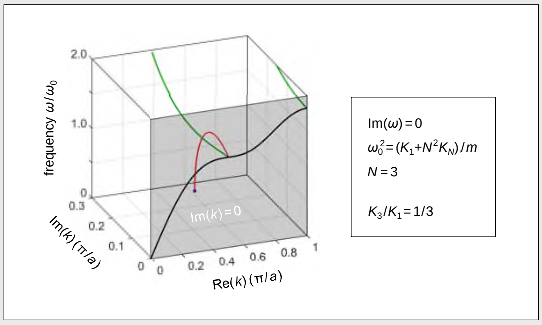

Y. Chen, J.L.G. Schneider, *et al.*, in preparation (2023)

Complex Phonon Band Structure

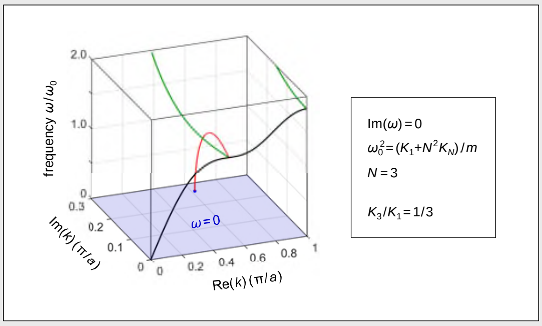

Y. Chen, J.L.G. Schneider, *et al.*, in preparation (2023)

Complex Phonon Band Structure

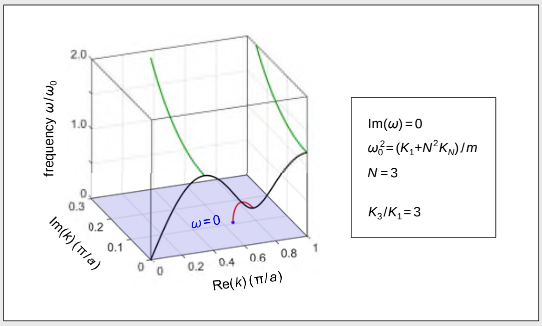

Y. Chen, J.L.G. Schneider, *et al.*, in preparation (2023)

Complex Phonon Band Structure

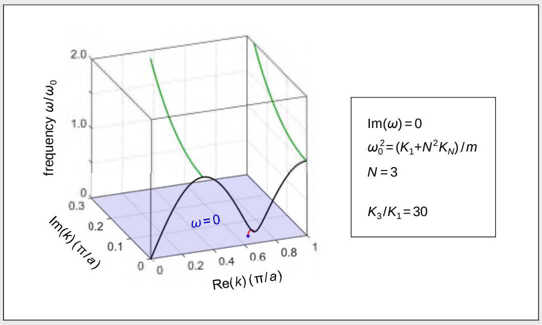

Y. Chen, J.L.G. Schneider, *et al.*, in preparation (2023)

We refer to these zero-frequency eigensolutions as **frozen evanescent phonons**. These solutions are static **oscillations** of the displacement field with **spatial period**

$$\lambda = \frac{2\pi}{\mathrm{Re}(k)} \to 3a = Na$$

and **decay length**

$$l = \frac{1}{\mathrm{Im}(k)} \to a\sqrt{3\frac{K_3}{K_1}} \to \infty$$

in the limit of strong nonlocal interactions, $K_3/K_1 \to \infty$.

Y. Chen, J.L.G. Schneider, *et al.*, in preparation (2023)

The solution of any specific problem for a **finite-size sample** is given by that linear superposition of the frozen phonon eigenmodes (of the **infinite system**) that matches the boundary conditions.

Here, non-Bloch solutions can additionally come into play.

Y. Chen, J.L.G. Schneider, *et al.*, in preparation (2023)

How in more General?

Martin Wegener

Any complex-valued **analytical function**

$$f(z) = f(x + \mathrm{i}y) = u + \mathrm{i}v$$

obeys the **Cauchy-Riemann** equations

$$\frac{\partial u}{\partial x} = \frac{\partial v}{\partial y}\,; \qquad \frac{\partial u}{\partial y} = -\frac{\partial v}{\partial x}$$

from which it follows that

$$\frac{\partial^2 u}{\partial x^2} = -\frac{\partial^2 u}{\partial y^2}$$

Martin Wegener

For a dispersion relation $\omega(k) = f(z)$ with a minimum at $\omega(k_{\mathrm{min}} + \mathrm{i}\,0) = \omega_{\mathrm{min}} + \mathrm{i}\,0 \to 0$, this equation reads

$$\frac{\partial^2(\mathrm{Re}(\omega))}{\partial(\mathrm{Re}(k))^2}(k_{\mathrm{min}}) = -\frac{\partial^2(\mathrm{Re}(\omega))}{\partial(\mathrm{Im}(k))^2}(k_{\mathrm{min}}) = \zeta > 0$$

and leads to a **frozen evanescent phonon decay length**

$$l = \frac{1}{\mathrm{Im}(k_{\mathrm{min}})} \to \sqrt{\frac{\zeta}{2\,\omega_{\mathrm{min}}}} \to \infty$$

Y. Chen, J.L.G. Schneider, *et al.*, unpublished (2023)

Complex Phonon Band Structure

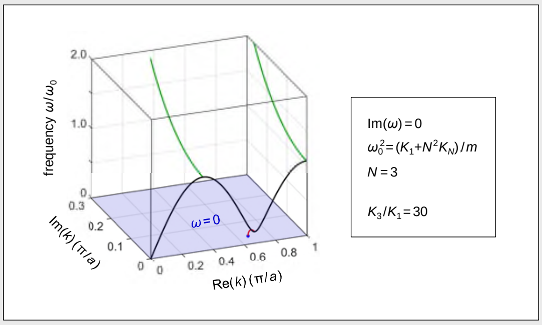

Y. Chen, J.L.G. Schneider, *et al.*, unpublished (2023)

Martin Wegener

Nonlocal Metamaterial Beam

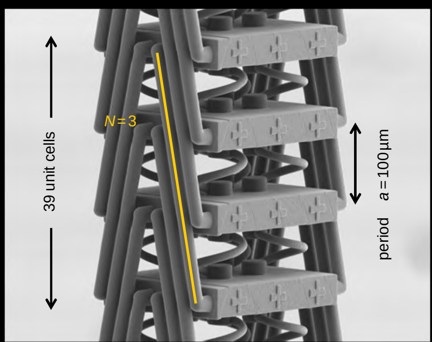

Y. Chen, J.L.G. Schneider, *et al.*, in preparation (2023)

Static Stretching Experiment

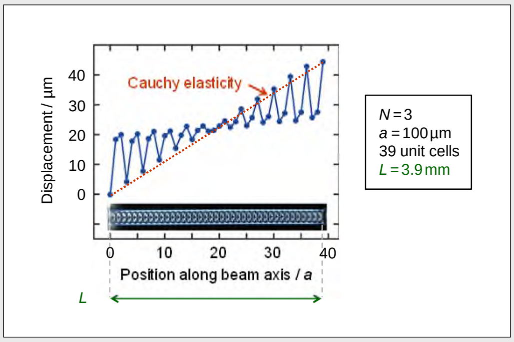

Y. Chen, J.L.G. Schneider, *et al.*, in preparation (2023)

Violation of Saint Venant's Principle

which can be used for remote mechanical sensing

Martin Wegener

Three review articles on mechanical metamaterials

M. Kadic *et al.*, Rep. Prog. Phys. 76, 126501 (2013)
M. Kadic *et al.*, Nature Rev. Phys. 1, 198 (2019)
R. Craster *et al.*, Rep. Prog. Phys. 86, 094501 (2023)

Martin Wegener

Acknowledgements

Martin Wegener

Involved group members @ KIT:

Dr. N. Maximilian Bojanowski (postdoctoral researcher)
Dr. Yi Chen (postdoctoral researcher)
Dr. Tobias Frenzel (PhD thesis)
Michael F. Groß (PhD thesis)
Dr. Vincent Hahn (PhD thesis)
Pascal Kiefer (PhD thesis)
Tobias Messer (PhD thesis)
Jonathan L.G. Schneider (PhD thesis)
Ke Wang (PhD thesis)

Collaborating groups:

Prof. Peter Gumbsch (Mechanical Engineering, KIT, Germany)
Prof. Sébastien R.L. Guenneau (Imperial College, London, UK)
Prof. Muamer Kadic (FEMTO-ST, Besancon, France)
Prof. Vincent Laude (FEMTO-ST, Besancon, France)
Prof. Changguo Wang (Harbin Institute of Technology, China)

Martin Wegener

DFG Deutsche Forschungsgemeinschaft
Excellence Strategy, EXC 2082

Baden-Württemberg

KIT

Carl Zeiss Stiftung

3D MATTER MADE TO ORDER

HEiKA

HELMHOLTZ RESEARCH FOR GRAND CHALLENGES
Excellence Networks, Phases 2 and 3

UNIVERSITÄT HEIDELBERG ZUKUNFT SEIT 1386

HELMHOLTZ RESEARCH FOR GRAND CHALLENGES
Materials Systems Engineering (MSE)

KSOP Karlsruhe School of Optics & Photonics

nanoscribe A BICO COMPANY

Hector Fellow Academy

MAX PLANCK SCHOOL of photonics

martin.wegener@kit.edu

Martin Wegener